

DOI: 10.1002/cmdc.200700151

# Virtual Screening for Selective Allosteric mGluR1 Antagonists and Structure–Activity Relationship Investigations for Coumarine Derivatives

Tobias Noeske,<sup>[a]</sup> Aigars Jirgensons,<sup>[b]</sup> Igors Starchenkovs,<sup>[b]</sup> Steffen Renner,<sup>[a, c]</sup> Ieva Jaunzeme,<sup>[b]</sup> Dina Trifanova,<sup>[b]</sup> Mirko Hechenberger,<sup>[a]</sup> Tanja Bauer,<sup>[a]</sup> Valerjans Kauss,<sup>[b]</sup> Christopher G. Parsons,<sup>[a]</sup> Gisbert Schneider,<sup>[c]</sup> and Tanja Weil\*<sup>[a]</sup>

A virtual screening study towards novel noncompetitive antagonists of the metabotropic glutamate receptor 1 (mGluR1) is described. Alignment-free topological pharmacophore descriptors (CATS) were used to encode the screening compounds. All virtual hits were characterized with respect to their allosteric antagonistic effect on mGluR1 in both functional and binding assays. Exceptionally high hit rates of up to 26% were achieved, confirming the applicability of this virtual screening concept. Most of the compounds were found to be moderately active, however, one potent and subtype selective mGluR1 antagonist, **13** ( $IC_{50}$ : 0.362  $\mu\text{M}$ ,  $SEM \pm 0.031$ ;  $K_i$ : 0.753  $\mu\text{M}$ ,  $SEM \pm 0.048$ ), based on a coumarine scaffold was discovered. In a following activity optimi-

zation program a series of coumarine derivatives was synthesized. This led to the discovery of potent (**60**,  $IC_{50}$ : 0.058  $\mu\text{M}$ ,  $SEM \pm 0.008$ ;  $K_i$ : 0.293  $\mu\text{M}$ ,  $SEM \pm 0.022$ ) and subtype selective (rmGluR5  $IC_{50}$ : 28.6  $\mu\text{M}$ ) mGluR1 antagonists. From our homology model of mGluR1 we derived a potential binding mode within the allosteric transmembrane region. Potential interacting patterns are proposed considering the difference of the binding pockets between rat and human receptors. The study demonstrates the applicability of ligand-based virtual screening for non-competitive antagonists of a G-protein coupled receptor, resulting in novel, potent, and selective agents.

## Introduction

G-protein coupled receptors (GPCRs) represent the largest family of cell-surface receptors involved in signal transmission.<sup>[1]</sup> More than 50% of the drugs on the market mediate their effect via GPCRs.<sup>[2,3]</sup> Based on sequence similarity, GPCRs can be subdivided into three groups: The rhodopsin/ $\beta$ -adrenergic receptors (family 1), the secretin receptors (family 2), and the metabotropic glutamate receptors (family 3).<sup>[4]</sup> In addition to metabotropic glutamate receptors (mGluRs), family 3 GPCRs comprise the GABA<sub>B</sub>,<sup>[5]</sup> the calcium-sensing,<sup>[6]</sup> vomeronasal,<sup>[7]</sup> pheromone,<sup>[8]</sup> and several putative taste receptors. These receptors are characterized by a large extracellular domain (ECD), a heptahelical domain (HD)—which is composed of seven transmembrane helices linked to each other by alternating extracellular and intracellular loops—and an intracellular domain (ICD) including the C terminus and the G-protein interaction sites. The extracellular amino-terminal domain contains a Venus flytrap module for orthosteric agonist binding.<sup>[9]</sup> This is in contrast to most other GPCRs where natural ligand binding occurs within the heptahelical domain.<sup>[10]</sup> The mGluR family consists of eight cloned subtypes mGluR1–8 and several splice variants.<sup>[11]</sup> Metabotropic glutamate receptors are further subdivided into three groups according to their sequence similarity and their mechanism of signal transduction.

Group 1 receptors (mGluR1 and mGluR5), are localized postsynaptically in the somatodendritic membrane and coupled to the activation of phospholipase C (PLC)<sup>[12]</sup> and, thus, are considered to be stimulatory. Although glutamate neurotransmission is primarily mediated by postsynaptic ligand-gated cation channels, for example, ionotropic glutamate receptors, it can also be regulated by mGluRs. According to previous studies, the mGluR1 receptor seems to be mainly involved in therapeutic opportunities such as stroke, brain injury,<sup>[13,14]</sup> and pain.<sup>[15,16]</sup> It was shown that the heptahelical domain of mGluRs provides a binding pocket for a novel class of ligands acting as allosteric

[a] T. Noeske, Dr. S. Renner, Dr. M. Hechenberger, T. Bauer, Dr. C. G. Parsons, Dr. T. Weil  
Merz Pharmaceuticals GmbH, Altenhöfer Allee 3, 60438 Frankfurt am Main (Germany)  
Fax: (+49) 69-1503188  
E-mail: tanja.weil@merz.de

[b] Dr. A. Jirgensons, Dr. I. Starchenkovs, I. Jaunzeme, D. Trifanova, Dr. V. Kauss  
Latvian Institute of Organic Synthesis, 21 Aizkraukles, Riga LV 1006 (Latvia)

[c] Dr. S. Renner, Prof. Dr. G. Schneider  
Johann Wolfgang Goethe-University, Institute of Organic Chemistry & Chemical Biology, Siesmayerstraße 70, 60323 Frankfurt am Main (Germany)

Supporting information for this article is available on the WWW under <http://www.chemmedchem.org> or from the author.

agonists or antagonists,<sup>[17]</sup> thus, modulating the activation of the receptor induced by an orthosteric agonist in a noncompetitive way. CPCCOEt was one of the first mGluR1 antagonists with low micromolar affinity.<sup>[18]</sup> Other mGluR1 antagonists such as R214127, LY456066, and EMTBPC have affinities down to low-nanomolar levels (their chemical structures are given in the Supporting Information).<sup>[19–21]</sup> The important role of allosteric antagonists of group 1 mGluRs in diseases involving neurodegeneration (for example, Alzheimer's and Parkinson's disease), anxiety, pain, epilepsy, and neuroprotection (stroke, ischaemia), and schizophrenia has been investigated before.<sup>[22–24]</sup>

So far, most known mGluR modulators were discovered by applying high throughput screening (HTS) technologies. Although HTS represents a main source for identifying novel hit compounds, it is associated with numerous pitfalls, for example, high investment, low hit rates, high number of false positives or false negatives. HTS is complemented by virtual screening concepts, which turned out to provide rapid and efficient techniques for selecting activity-enriched subsets of screening candidates.<sup>[25]</sup> In this study we have applied virtual screening to finding novel mGluR1 antagonists by a ligand-based approach, that is, a topological pharmacophore search (CATS).<sup>[26]</sup> Topological descriptors were calculated from the 2D-structure of known mGluR1 antagonists to avoid problems related to conformational flexibility as the preferred binding mode of allosteric mGluR1 antagonists is still unknown. A set of virtual hits were obtained and pharmacologically characterized and the most active compound served as the starting point for a subsequent lead optimization program. A focused library was designed, and mGluR1 antagonists with an improved potency and high selectivity towards mGluR5 were obtained. Moreover, two representatives potentially antagonizing the mGlu1 receptor were placed into the allosteric binding pocket of our own mGluR1 homology model, which differs from previously reported models.<sup>[21,27]</sup> We identified

amino acid residues presumably interacting with pivotal ligand features.

## Results and Discussion

### Virtual Screening

Six known mGluR1 antagonists served as reference compounds ("seeds") for similarity searching in a commercially available compound collection (Gold Collection of Asinex Ltd.<sup>[28]</sup>) (Figure 1). Each reference compound in turn served as the query structure for the CATS search, and the remaining five

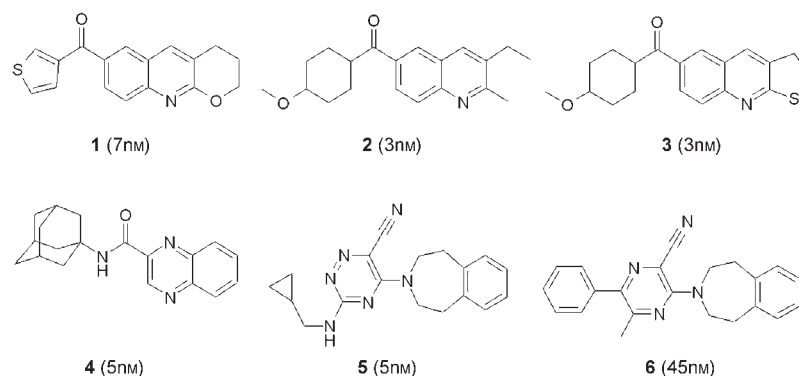


**Figure 1.** Seed structures used for virtual screening. The functional activities of molecules 1–6 for mGluR1 antagonism are given. Molecules 1–3 closely resemble R214127,<sup>[19]</sup> molecules 5 and 6 are EM-TBPC analogues.<sup>[20]</sup>

**Table 1.** Activity of the compounds found by virtual screening.<sup>[a]</sup>

Scoring list	Rank	Chemical Structure	No.	mGluR1 IC <sub>50</sub> [ $\mu$ M]	mGluR1 K <sub>i</sub> [ $\mu$ M]
1	3		7	7.9 ( $\pm$ 2.5)	> 40
2	2		12	13.5 ( $\pm$ 7.0)	25.3 ( $\pm$ 5.1)
3	2		13	0.36 ( $\pm$ 0.03)	0.75 ( $\pm$ 0.05)
6	3		19	12.9 ( $\pm$ 1.0)	21.6 ( $\pm$ 3.6)
1	77		27	13.2 ( $\pm$ 4.1)	> 40
2	41				
3	72				
1	32		28	11.1 ( $\pm$ 3.0)	> 40
2	18				
3	95				

[a] Only hits with IC<sub>50</sub> < 15  $\mu$ M are shown. The first two columns indicate the seed compound on which the search was based and the position of the test compounds in the corresponding scoring list. Activities are given as mean values of two independent experiments performed in quadruplicate (binding, K<sub>i</sub>) or sextuplicate (functional, IC<sub>50</sub>).

molecules were mixed with the library compounds. This database “spiking” was done to gain an idea of the relevance of the obtained virtual hit lists<sup>[29]</sup> (see Experimental Section). For each run, the CATS-program was prompted to create a ranked list of the 100 most similar screening compounds. This resulted in six such virtual hit lists or scoring lists (Table 1). From each list the top-scoring five compounds were selected. In addition, we picked all virtual hits that occurred in at least three of the six hit lists, irrespective of their rank. In total, 38 compounds were ordered, 23 were delivered, and their pharmacological profile was characterized. Table 1 only shows the most potent compounds that were identified. A complete list of all compounds that were tested is provided in the Supporting Information (Table S1). Among those compounds, some structurally similar ones with respect to their seed compounds (1–3) such as 11, 25, in particular 26, and test compound 14 (seed compound 4) were identified (Supporting Information Table S1), which is confirmed by their CATS similarity values (not shown). However, the majority of the test compounds were structurally distinct from their seed compounds. The pharmacological profile of compounds 7–29 was characterized using in vitro binding and functional assays. In the binding assay, the displacement of binding of the known noncompetitive mGluR1 antagonist [<sup>3</sup>H]-3-Ethyl-2-methyl-quinolin-6-yl)-(4-methoxy-cyclohexyl)-methanone ([<sup>3</sup>H]-2) (Figure 1), a tritiated analogue of 2, was measured. In the functional assay, changes in the inositol phosphate (IP<sub>3</sub>) level were recorded. For pharmacological screening purpose binding constants  $K_i$  (the displacement of radioligand as % of control was measured and  $K_i$  was calculated; Supporting Information) and inhibition constants ( $IC_{50}$ ) have been determined by dose response curves with a few concentrations, whereas for SAR studies full dose response curves have been conducted (see Supporting Information). One compound was found to be highly active ( $<1 \mu\text{M}$ ), and five compounds were moderately active with  $IC_{50}$  values between 1–15  $\mu\text{M}$  in the functional assay. Seven compounds exhibited low activity (15–40  $\mu\text{M}$ ), and ten compounds were found to be inactive ( $IC_{50} > 40 \mu\text{M}$ ). This resulted in an overall hit rate of approximately 26%, determined by taking into account all compounds with an  $IC_{50}$  below 15  $\mu\text{M}$ . In general, higher activities were found in the functional assay than in the binding assay, which could have different reasons, for example, the existence of another binding site, which cannot be accessed by the radioligand but can be by test compounds thus revealing significantly higher functional potency than binding potency (for example, 42) or overlapping binding sites. Interestingly, compound 13 was found to bind to the allosteric site of the mGluR1 receptor with an  $IC_{50}$  value in the nanomolar range and significantly inhibits receptor activation induced by the orthosteric agonist (*R,S*)-3,5-dihydroxy-phenylglycine (DHPG, Figure 2). It displaced the binding of [<sup>3</sup>H]-2 with a  $K_i$  value of 0.811  $\mu\text{M}$  (standard error of the mean, SEM,  $\pm 0.048$ ) and inhibits DHPG-induced intracellular IP<sub>3</sub> formation with an  $IC_{50}$  value of 0.362  $\mu\text{M}$  (SEM  $\pm 0.031$ ). Moreover, compound 13 is subtype selective as no affinity towards mGluR5, the closest related subtype according to sequence similarity, was observed (Figure 3). This is demonstrated in a mGluR5 binding assay by applying the potent and se-

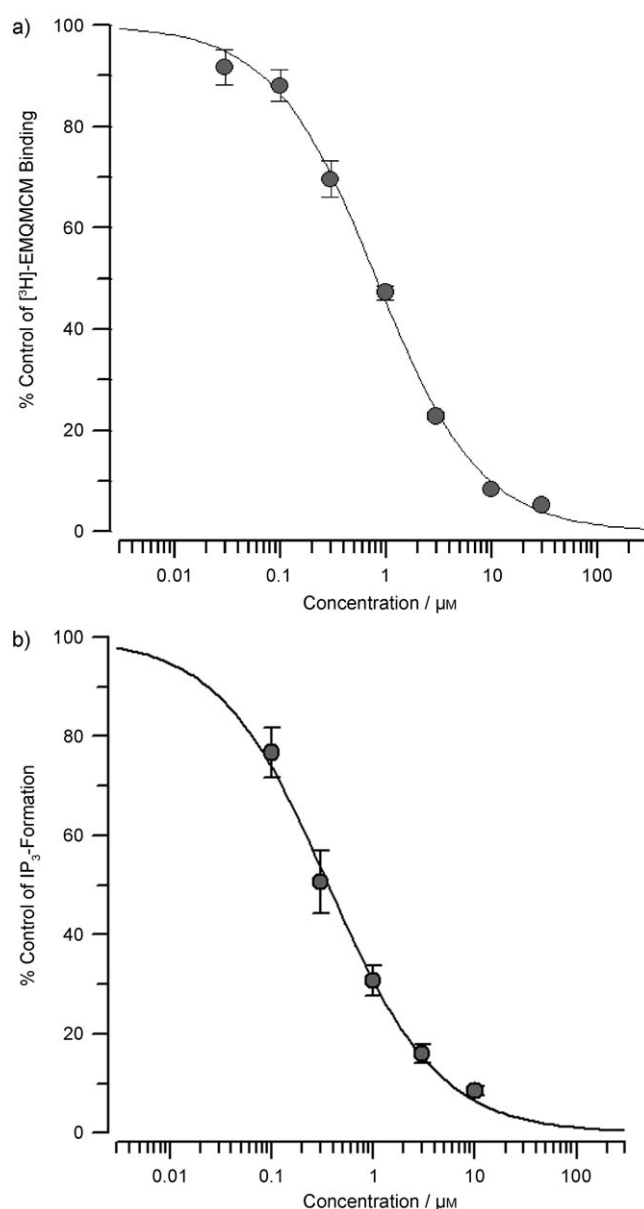


**Figure 2.** Compound 13 is a noncompetitive antagonist of the mGluR1 receptor. It displaces [<sup>3</sup>H]-EMQMCM binding to the allosteric mGluR1 site with an  $IC_{50}$  value of 0.753  $\mu\text{M}$  (SEM  $\pm 0.048$ ) and inhibits DHPG-induced intracellular IP<sub>3</sub> formation with an  $IC_{50}$  value of 0.362  $\mu\text{M}$  (SEM  $\pm 0.031$ ). Results represent mean values of two independent experiments performed in quadruplicate (binding) or sextuplicate (functional), respectively.

lective mGluR5 antagonist [<sup>3</sup>H]-2-(3-methoxy-phenylethynyl)-6-methyl-pyridine ([<sup>3</sup>H]-M-MPEP).<sup>[30]</sup> Tritiated M-MPEP itself is displaced by the known mGluR5 antagonist MPEP as shown in Figure 3.

### Synthesis of a focused coumarine library

Compound 13 is based on a coumarine scaffold and to the best of our knowledge no interactions of coumarine derivatives with group 3 GPCRs have been reported before.<sup>[31]</sup> Synthesis strategies were explored to elaborate a structure–activity relationship around this scaffold and to improve its activity fur-

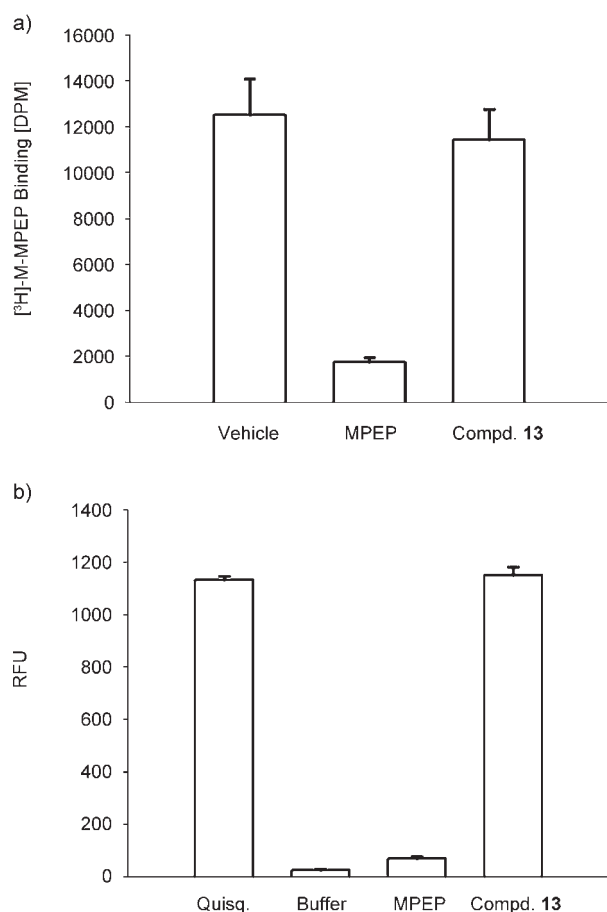


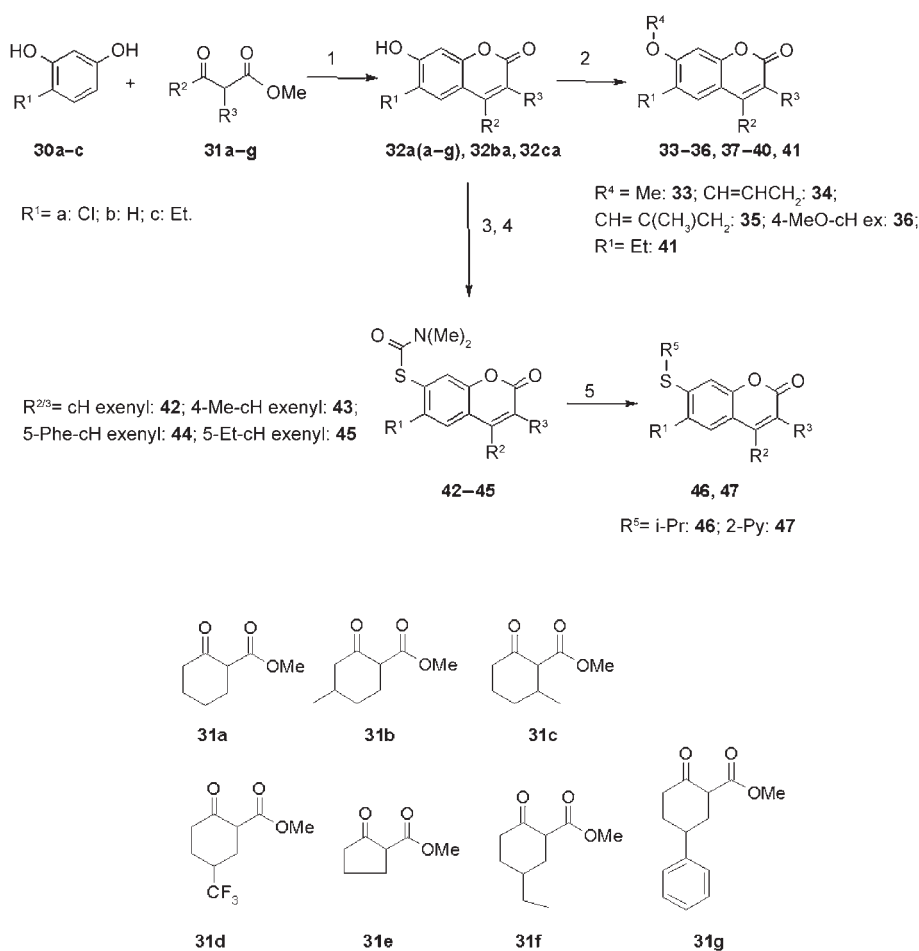
**Figure 3.** In contrast to MPEP (10  $\mu\text{M}$ ), compound **13** (10  $\mu\text{M}$ ) does not displace the binding of [ $^3\text{H}$ ]-M-MPEP (5 nM) to the allosteric site of the mGlu5 receptor nor does it inhibit quisqualate (100 nM) induced intracellular  $\text{Ca}^{2+}$  release in rat cortical astrocytes (MPEP: 1  $\mu\text{M}$ ). Results are mean values of two independent experiments conducted in duplicate (M-MPEP binding) or quintuplicate (calcium-flux). Error bars indicate SEM.

ther. Pechmann condensation of resorcinols **30 a–c** with cyclic  $\beta$ -ketoesters **31 a–g** (Scheme 1 b) was used to prepare hydroxycoumarin derivatives **32 a(a–g)**, **32 ba**, and **32 ca** (Scheme 1 a, examples see Supporting Information). Alkylation at the hydroxy group of compounds corresponding to general formula **32** led to alkyl- and vinyl-aryl ethers **33–36**, **37–40**, and **41**. A reaction of hydroxyresorcinols **32** with *N,N*-dimethylthiocarbonylchloride and subsequent Newman-Kwart rearrangement<sup>[33,34]</sup> gave mercaptocoumarin derivatives **42–45**. The carbonyl group in compound **42** was cleaved and the mercapto group was alkylated or arylated to give compounds **46** and **47**, respectively. 7-Hydroxycoumarins **32 aa** and **32 ba** were nitrated at the free *ortho* position of phenolic hydroxy group and subsequently alkylated at the hydroxy group to obtain 8-nitro- and 6-nitrocoumarin derivatives **48** and **53**. Hydrogenation of the nitro group of compounds **48** and **53** followed by acylation gave coumarin derivatives **49–52** and **54** (Scheme 2 a). The Knoevenagel condensation of *ortho*-hydroxybenzaldehydes **55 a–d** with ethyl 3-adamantan-1-yl-3-oxopropionate (**56**) in the presence of piperidine in ethanol was used to pre-

pare substituted 3-(adamantane-1-carbonyl)-chromen-2-ones **57–60** (Scheme 2 b).<sup>[35]</sup>

### Structure–activity relationship (SAR)

Based on our primary hit compound **13**, three parts of the molecule were chosen for structural modifications. A small library where  $\text{R}^1$  was systematically varied led to the discovery of **42** yielding an  $\text{IC}_{50}$  value of 123 nM (Table 2). The introduction of an *iso*-propoxy or a thioamide group at  $\text{R}^1$  turns out to be favorable to achieve highly active mGluR1 antagonists. Other hydrophobic, aromatic ether or thioether substituents at  $\text{R}^1$  gave only moderately active coumarin derivatives whose activities were found to vary between 1 and 10  $\mu\text{M}$  in the functional mGluR1 assay (Table 2). In the next step, the *iso*-propoxy group at  $\text{R}^1$  of **13** was kept fixed and position  $\text{R}^2$  was varied (Table 3). In particular, hydrogen bond acceptors and donors were introduced (**49–52**). A moderate antagonizing effect was observed in the functional assay whereas in the binding assay, only low affinities were found. Therefore, the optimal substituents at  $\text{R}^2$  seem to be small and nonpolar, for example, hydrogen. Any effort towards increasing affinity with functional groups at  $\text{R}^2$  failed. Table 4 shows that the introduction of alkyl- (**41**), amido- (**54**), hydrogen (**61**), or nitro groups (**53**) in  $\text{R}^4$  led to a decrease in the functional activity and therefore, they could not be regarded as an alternative for the chloro substituent of **13**. Then, the carbocycle next to the lactone ring was varied with respect to size and substitution pattern (Table 5). The introduction of a methyl substituent (**37**) is followed by an increase in functional activity to 200 nM whereas the 7-methyl substituent (**38**) significantly reduced functional activity. Interestingly, after exchange of the *iso*-propoxy group of **37** (199 nM) by dimethyl-thiocarbamic acid substituent (**43**, 885 nM), which was found to be the optimal group in the absence of the 7-methyl group before (**42**, 123 nM, Table 2), a decrease in functional activity was obtained for **43** in the presence of the 9-methyl substituent. Other modifications such as 8- $\text{CF}_3$  (**39**), 8-ethyl substituents (**45**), and a reduction in ring size (**40**) were well tolerated and only minor activity changes were observed. The activity data of **37**, **39**, and **43** suggest that there exists a hydrophobic pocket within the mGluR1 receptor, which could be further explored by changing the substitution pattern at the coumarin core. Therefore, an adamantyl substituent was introduced and connected by a carbonyl group (Table 6), and only the substituent  $\text{R}^1$  at the coumarin scaffold was kept. By using this modification, antagonists with an improved activity down to 30 nM were obtained (**57–60**). Interestingly, for this structural class better correlations between binding and functional assays were achieved. The main SAR findings of Tables 1–6 are summarized in Figure 4. Red denotes the presence of a hydrogen acceptor group, orange corresponds to hydrophobic and acceptor groups whereas the gray color represents a hydrophobic substituent. In the next step, a homology model of mGluR1 was developed to get an idea of the potential binding mode of selective coumarin antagonists presented above.



**Scheme 1.** a) Reagents and conditions: 1)  $\text{H}_2\text{SO}_4$ , RT.; 2)  $\text{R}^4\text{X}$ ,  $\text{K}_2\text{CO}_3$  or  $\text{CsCO}_3$ , acetone or DMFA, RT. or heating; 3)  $\text{Me}_2\text{NC(=S)Cl}$ , DABCO, DMFA; 4) *N,N*-Diethylaniline, 120 °C; 5) 1N MeONa, MeOH, RT overnight, then  $\text{R}^5\text{Br}$ ,  $\text{K}_2\text{CO}_3$ , RT for **46**, 160 °C for **47**. b)  $\beta$ -Ketoesters used for Pechmann condensation in part a.

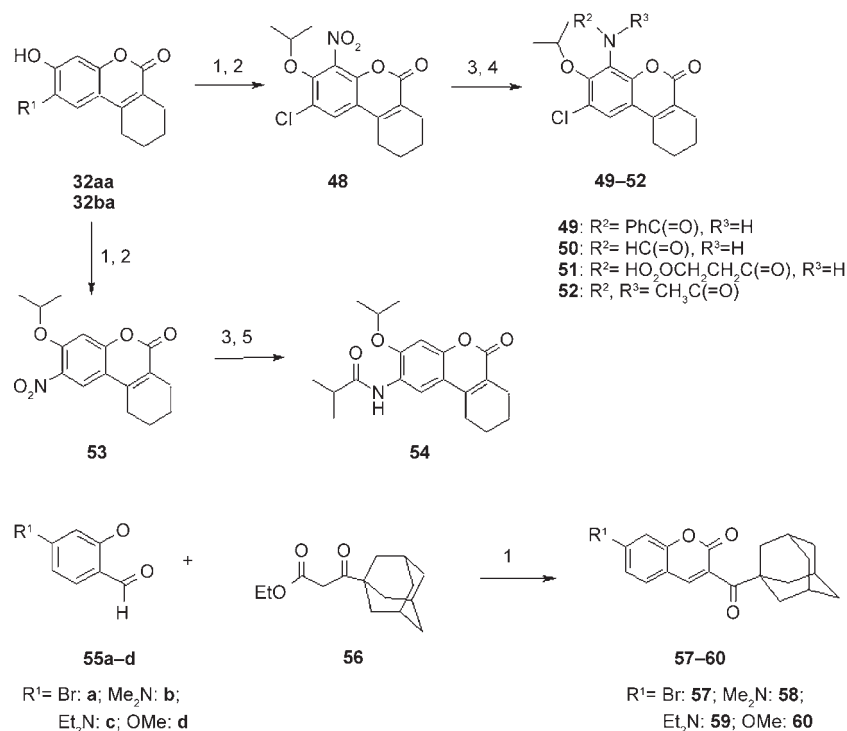
### Binding mode of different coumarin derivatives

The ligands were manually placed into the transmembrane region in proximity to the pocket where 11-*cis*-retinal was found in bovine rhodopsin.<sup>[36]</sup> As preliminary experiments with automated docking methods did not lead to reasonable results, we decided to place the ligands manually in a way most consistent with the obtained SAR data and mutational results from literature (see the following details), followed by an energy minimization. We wish to stress that all presented binding modes are hypotheses fitting best to our experimental data rather than extensively evaluated and confirmed results. As starting point for the placement of the molecules in the binding site we used data on differences in functional activity of the molecules between rat and human mGluR1. Of several ligands for which functional activity in human mGluR1 was also measured (**13**, **33**, **36–42**, **47**, **49**, **51**, **54**, **59**, **60**, **61**), all but **41** showed lower activity on the human receptor. This difference was attributed to the single amino acid difference between rat and human receptors within the ligand-binding region: V757 (5.47 according to the numbering scheme of Ballesteros<sup>[32]</sup>) in rat versus L757 in human. We have selected the hydrophobic unsaturated ring as the most likely candidate to

interact with this amino acid. Figure 5a shows the predicted binding mode of **13** in the binding pocket of mGluR1. The unsaturated ring is in contact with the rat selective V757 (5.47), which is surrounded by further hydrophobic residues V753 (5.43) and P756 (5.46) that form a hydrophobic cluster. In the homology model, the central lactone group of the coumarin core interacts as an acceptor forming two hydrogen bonds with R661 (3.29) and N747 (45.51). The hydrophobic *iso*-propoxy substituent of **13** interacts with the hydrophobic residues I745 (45.49) and V664 (3.32) whereas the ether group seems to be involved in forming a hydrogen bond with T815 (7.39). Replacing the *iso*-propoxy group with a dimethylthiocarbamyl group resulted in increased activity (**42**, with  $\text{IC}_{50} = 0.12 \mu\text{M}$ , compared to **13** with  $\text{IC}_{50} = 0.36 \mu\text{M}$ ). This might be explained by the formation of a stronger hydrogen bond to T815 (7.39) by the dimethylthiocarbamyl group compared to the *iso*-propoxy group. Substituents at the chlorine site of **13** might interact with V664 (3.32)

and V819 (7.43). In comparison to the binding mode of **13**, the receptor model suggests that for all ligands bearing an adamantyl substituent next to the lactone ring (**57–60**) there is not sufficient space for the adamantyl group in the subpocket covered by the unsaturated ring of **13**. Thus, an alternative binding mode was proposed for the adamantyl-containing ligands, illustrated by **60** (Figure 5b). Here the adamantyl group fills the same part of the pocket as the unsaturated ring in **13**. The oxygen of the carbonyl linker of **60** is involved in the hydrogen bond cluster containing R661 (3.29), and the oxygen acceptor in the ring from the coumarin core forms a hydrogen-bonding interaction with T815 (7.39) (see Figure 6).

Both ligands **13** and **60** were found to be subtype-selective against mGluR5. According to the homology model, the two binding sites of the receptor subtypes were very similar. Only four residues differed near the proposed binding site: positions 3.32 (mGluR1 V664 versus mGluR5 I650), 3.36 (S668 versus P654), 5.47 (V757 versus L743), 7.39 (T815 versus M801). The unfavorable effect of L replacing V on position 5.47 was already observed experimentally in this study comparing human and rat mGluR1. The same effect might contribute to the selectivity over mGluR5. M instead of T at position 7.39 in mGluR5



**Scheme 2.** a) Reagents and conditions: 1) HNO<sub>3</sub>, AcOH, RT; 2) *i*PrBr, K<sub>2</sub>CO<sub>3</sub>, DMFA, 50 °C; 3) H<sub>2</sub>, 10% Pd/C; EtOH, RT; 4) for **49**: PhC(=O)Cl, Py, THF, RT; for **50**: HCO<sub>2</sub>H, reflux; for **51**: succinic anhydride, xylenes, 140 °C; for **52**: Ac<sub>2</sub>O, reflux; 5) *i*PrC(=O)Cl, Py, THF, RT. b) Reagents and conditions: 1) piperidine, ethanol reflux.

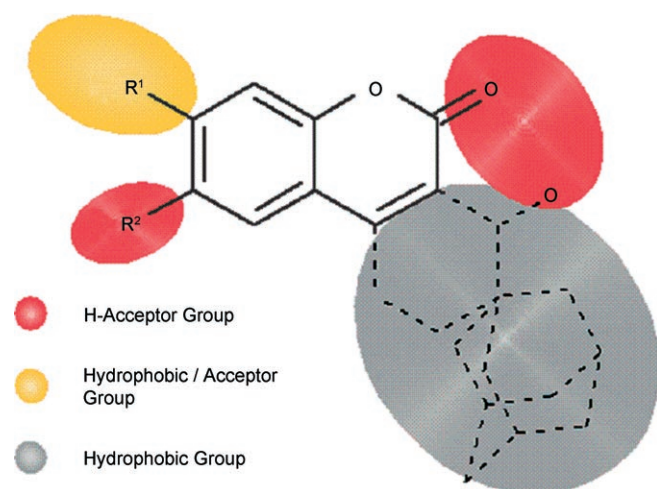


**Figure 4.** Visualization of the SAR results for coumarines. Bold lines indicate the common core and dashed lines denote hydrophobic moieties condensed or attached to the scaffold.

might prevent binding of the ligands by its more voluminous sidechain that also cannot form the hydrogen-bonding interaction that was proposed for all our ligands (Figure 5). The larger sidechains of I in mGluR5 compared to V at position 3.32 and P instead of S at 3.36 might also contribute to the selectivity by steric hindrance. The proposed binding pocket of **13** and **60** is located in a similar region compared with the negative allosteric mGluR1 modulator EM-TBPC, for which mutational data was published before.<sup>[21]</sup> EM-TBPC is assumed to interact with

V757 (5.47), W798 (6.48), F801 (6.51), Y805 (6.55), T815 (7.39), which are all in proximity to **13** and **60**. Mutation of N747 (45.51) and N750 (45.54) to alanine resulted in an increased effect of EM-TBPC, which might be caused by the lack of a hydrogen-bond interaction partner of EM-TBPC. These findings are consistent with a direct interaction of N747 (45.51) with our ligands. For rmGluR5 it was also shown that mutation of R647 (3.29) (R661 in mGluR1) to alanine increased the activity of the mGluR5 negative allosteric modulator MPEP.<sup>[37]</sup> This is consistent with a potential direct interaction of arginine at 3.29 (R661 in mGluR1 and R647 in rmGluR5) with bound ligands. These data support our hypothesis for the binding mode of **13** and **60**. Furthermore, the existence of different binding modes within the pocket could serve as an explanation for the observed differences in the functional and binding assay results as well as the failed attempt to find a quantitative SAR.

## Conclusion

We have presented the successful applicability of a similarity search based on topological CATS-descriptors for the identification of novel allosteric mGluR1 antagonists. One highly active antagonist based on a coumarin scaffold was found, which was subjected to a hit optimization program. A focused coumarin library was designed, which led to novel antagonists with an improved potency below 100 nM. A homology model was developed to which different coumarin antagonists were manually docked. A switch in the binding mode of different antagonists was predicted depending on the type and the position of the substituent at the coumarin core.

## Experimental Section

### Computational Methods

**Datasets.** The Asinex Gold Collection provided by Asinex<sup>[28]</sup> was used in sd-format for virtual screening purposes. This external compound library is continuously being updated and we applied the versions of February 2003 (194,598 entries) and October 2003 (201 304 entries). Apart from the 2D-chemical structures they include predicted Lipinski rule properties and some ADMET properties. A reference database containing 212 compounds was assembled by manually collecting already published structures of non-competitive mGluR1 antagonists from publications and patents.

**Table 2.** Variation of R<sup>1</sup>.

	Structure	rmGluR1 IC <sub>50</sub> [μM]	rmGluR1 K <sub>i</sub> [μM]
13		0.36 (±0.03)	0.75 (±0.05)
33		1.95 (±0.22)	2.94 (±0.36)
34		4.10 (±0.60)	14.2 (±0.14)
35		5.11 (±0.70)	31.94 (±0.82)
36		3.28 (±0.28)	8.27 (±1.27)
42		0.12 (±0.007)	2.73 (±0.002)
46		1.94 (±0.29)	10.86 (±0.09)
47		5.35 (±0.90)	28.15 (±0.50)

These molecules cover a broad range of activity (1 nM to ≈ 10 μM) and represent various different chemical core structures.

**CATS-2D similarity search.** The CATS descriptor is a topological atom-pair descriptor and has been reported earlier.<sup>[26]</sup> As it is based on the two-dimensional structure of a molecule it circumvents problems derived from conformational flexibility. Topological information of a molecule is encoded by assigning each atom (node) to one of the following generalized atom types: hydrogen-bond donor (D), hydrogen-bond acceptor (A), positively charged (P), negatively charged (N) or lipophilic (L). Atoms, which do not belong to one of the five mentioned potential pharmacophore point groups, are not taken into account. Atom pairs denote the shortest distance connecting two nodes. The frequencies of all 15 possible atom pairs of CATS types (DD, DA, etc.) are determined and the resulting histogram is divided by the number of nonhydrogen atoms in the molecule to get a scaled vector.<sup>[38]</sup> The CATS-similarity (expressed by the euclidian distance measure) is defined by the degree to which the topological pharmacophore descriptors of two atoms match. The output of a CATS run is a list of all library compounds ranked by descending order according to the CATS-similarity of the test compound towards the reference compound

which is here referred to as "seed compound". Six molecules from the reference database (Figure 1) have been selected manually according to structural diversity and high potency serving as seed compounds. The test compounds and the seed compounds have been prepared for similarity search by removing all hydrogen atoms using CLIFF software (Molecular Networks GmbH, Erlangen, Germany). Intramolecular distances up to 10 bonds were considered in this study, leading to a 150 (10×15) dimensional vector representation of each molecular compound.

#### Pharmacological Methods

**Membrane preparation (cerebellum and cortex).** Male Sprague-Dawley rats (approx. 200–250 g) were anesthetized and decapitated. Cerebelli (forebrains for cortex preparation) were removed and homogenized (Ultra Turrax, 8 strokes, 600 rpm) in 0.32 M Sucrose. The suspension was centrifuged at 1,500 g for 4 min using a Sorvall Discovery 90 SE ultracentrifuge (Kendro Laboratory Products GmbH, Langensfeld, Germany). Supernatant was removed and centrifuged at 20,800 g for 20 min. The resulting pellet was resuspended in ice-cold distilled water and centrifuged at 7,600 g for another 20 min. Supernatant and loosely associated flocculent membrane material (buffy coat) were removed by gentle trituration of the pellet and centrifuged at 75,000 g for 20 min. Supernatant was discarded and the membrane pellet was resuspended by sonication in TrisBuffer (5 mM,

pH 7.4) and afterwards centrifuged at 75,000 g for 20 min. The last step was repeated twice and membranes were resuspended in TrisBuffer (50 mM, pH 7.5). The concentration of protein was determined by the Lowry protein assay with bovine serum albumin as standard.<sup>[39]</sup> Membranes were stored frozen at –24 °C, thawed on the day of the assay, and washed, and centrifuged once again at 75,000 g for 20 min. All centrifugation steps were carried out at 4 °C.

**[<sup>3</sup>H]-2 Binding assay.** After thawing, membranes were washed once with ice-cold binding buffer containing 50 mM Tris-HCl, pH 7.5. Binding assays were performed at RT in quadruplicate on 96-well format plates using fixed concentrations of the test compound (10 μM). The assay was incubated for 1 h in the presence of 1 nM [<sup>3</sup>H]-2 and membranes (0.8 mg mL<sup>-1</sup>) and nonspecific binding was estimated using 30 μM (3-Ethyl-2-methyl-quinolin-6-yl)-(4-hydroxycyclohexyl)-methanone.<sup>[28]</sup> Directly after transferring the reaction volume onto a 96-well multiscreen plate with glassfiber filter 0.22 μm (Millipore GmbH, Eschborn, Germany) binding was terminated by rapid filtration using a multiscreen vacuum manifold (Mil-

Table 3. Variation of R <sup>2</sup> .			
	Structure	rmGluR1 IC <sub>50</sub> [ $\mu$ M]	rmGluR1 K <sub>i</sub> [ $\mu$ M]
49		6.67 ( $\pm$ 1.19)	70.69 ( $\pm$ 2.04)
50		1.33 ( $\pm$ 0.16)	16.56 ( $\pm$ 0.76)
51		4.94 ( $\pm$ 0.65)	34.03 ( $\pm$ 0.74)
52		3.16 ( $\pm$ 0.31)	17.53 ( $\pm$ 0.17)

Table 4. Variation of R <sup>4</sup> .			
	Structure	rmGluR1 IC <sub>50</sub> [ $\mu$ M]	rmGluR1 K <sub>i</sub> [ $\mu$ M]
41		2.52 ( $\pm$ 0.24)	2.63 ( $\pm$ 0.05)
54		3.95 ( $\pm$ 0.41)	66.24 ( $\pm$ 1.15)
61		6.79 ( $\pm$ 0.92)	36.03 ( $\pm$ 1.26)
53		0.27 ( $\pm$ 0.088)	7.54 ( $\pm$ 0.07)

lipore GmbH, Eschborn, Germany). Afterwards, filters were washed three times with ice-cold assay-buffer and Ultima-Gold<sup>TM</sup> MV Scintillation Cocktail (Packard Bioscience, Groningen, The Netherlands) was added. After 14 h–16 h radioactivity was counted in a MicroBe-

vortexed before radioactivity was determined by conventional liquid scintillation counting (MicroBeta<sup>®</sup>Trilux, Perkin-Elmer Life Sciences GmbH, Rodgau-Jügesheim, Germany). Unless otherwise stated, all reagents were obtained from Sigma.

ta<sup>®</sup>Trilux (Perkin-Elmer Life Sciences GmbH, Rodgau-Jügesheim, Germany).

**Inositol phosphate determination.** After 6 DIV, the culture medium was replaced completely with inositol free DMEM (MP Biomedicals, Eschwege, Germany) containing [<sup>3</sup>H]-myo-inositol (Perkin-Elmer Life Sciences GmbH, Rodgau-Jügesheim, Germany) at a final concentration of 0.5  $\mu$ Ci/100  $\mu$ L/well and incubated for a further 48 h. The culture medium in each well was replaced with 100  $\mu$ L Locke's buffer (plus 20 mM LiCl, pH 7.4) and incubated for 15 min at 37 °C. Locke's buffer was replaced with agonists/antagonists/putative mGluR1 ligands in Locke's buffer and incubated for 45 min. These solutions were then replaced with 100  $\mu$ L 0.1 M HCl in each well and incubated for a further 10 mins on ice to lyse the cells. The 96-well plates can be frozen at -20 °C at this stage until further analysis. Homemade resin exchange columns were prepared as follows: Empty Bio-Spin Chromatography columns (Biorad Laboratories GmbH, München, Germany) were plugged with filter paper before filling with 1.1–1.3 mL of resin (AG1-X8 Biorad, 140-14444) suspended in 0.1 M formic acid (24 g resin per 50 mL acid). The formic acid was allowed to run out before sealing the syringe tips and filling with 200–300  $\mu$ L of 0.1 M formic acid before storage at 4 °C.

On the day of assay, columns were washed with 1 mL of 0.1 M formic acid followed by 1 mL of distilled water. Then the contents of each assay well were added to one column and washed with 1 mL distilled water followed by 1 mL of 5 mM Sodium tetraborate/60 mM sodium formate. Thereafter, the retained radioactive inositol phosphates were eluted with 2  $\times$  1 mL of 1 M ammonium formate/0.1 M formic acid into 24-well visiplates. Scintillation liquid (1.2 mL UltimaFlow AF, Perkin-Elmer) was added to each well, the plate sealed and

**Table 5.** Variation at position R<sup>3</sup>.

	Structure	rmGluR1 IC <sub>50</sub> [μM]	rmGluR1 K <sub>i</sub> [μM]
37		0.20 (±0.017)	0.69 (±0.047)
38		1.21 (±0.09)	0.91 (±0.131)
39		0.57 (±0.052)	2.98 (±1.05)
40		0.49 (±0.119)	3.95 (±0.23)
43		0.89 (±0.062)	5.24 (±0.52)
44		< 100	< 100
45		< 100	23.43 (±0.37)

**Table 6.** Variation of R<sup>1</sup> of adamantyl-substituted coumarin derivatives.

	Structure	rmGluR1 IC <sub>50</sub> [μM]	rmGluR1 K <sub>i</sub> [μM]
57		0.25 (±0.053)	0.43 (±0.049)
58		–	0.03 (±0.011)
59		–	0.04 (±0.004)
60		0.06 (±0.008)	0.29 (±0.022)

**[<sup>3</sup>H]-M-MPEP Binding Assay.** After thawing, cortex membranes were washed four times with ice-cold binding buffer containing 50 mM Tris-HCl, pH7.5. Binding assays were performed at RT in duplicate using fixed concentrations of the test compound (10 μM). The assay was incubated for 1 h in the presence of radiotracer (5 nM) and membranes (1.2 mg mL<sup>-1</sup>), and nonspecific binding was estimated using 10 μM MPEP. Binding was terminated by rapid filtration through GF 52 glass-fiber filters (Schleicher&Schuell, Dassel, Germany) using a 1225 Sampling Manifold (Millipore GmbH, Eschborn, Germany). Filters were washed twice with ice-cold assay-buffer and transferred to scintillation vials. After addition of Ultima-Gold™ MV (Packard Bioscience, Groningen, The Netherlands) radioactivity collected on the filters was counted in a 1500 Tri-Carb Packard Scintillation Counter.

**Calcium FLIPR studies.** Cultured astrocytes expressed mGluR5 receptors as shown by immunostaining. The increase of intracellular calcium after stimulation with the mGluR5 agonist DHPG or L-quisqualate was measured using the fluorometric imaging plate reader (FLIPR) and the Ca-Kit. Prior to addition of agonist or antagonist the medium was aspirated and cells were loaded for 2 h at RT with 150 μL of loading buffer consisting of a calcium-sensitive dye (MD # R8033) reconstituted in sodium chloride (123 mM), potassium chloride (5.4 mM), magnesium chloride (0.8 mM), calcium chloride (1.8 mM), D-glucose (15 mM), and HEPES (20 mM), pH7.3. Subsequently, plates were transferred to FLIPR to detect calcium increase with the addition of DHPG (300 μM) or L-quisqualate (100 nM) measured as relative fluorescence units (RFU). If antagonists were tested, these compounds were preincubated for 10 min at RT before addition of the respective agonist.

### Acknowledgements

The authors thank Aleksandrs Gutcaits (Institute of Organic Syn-

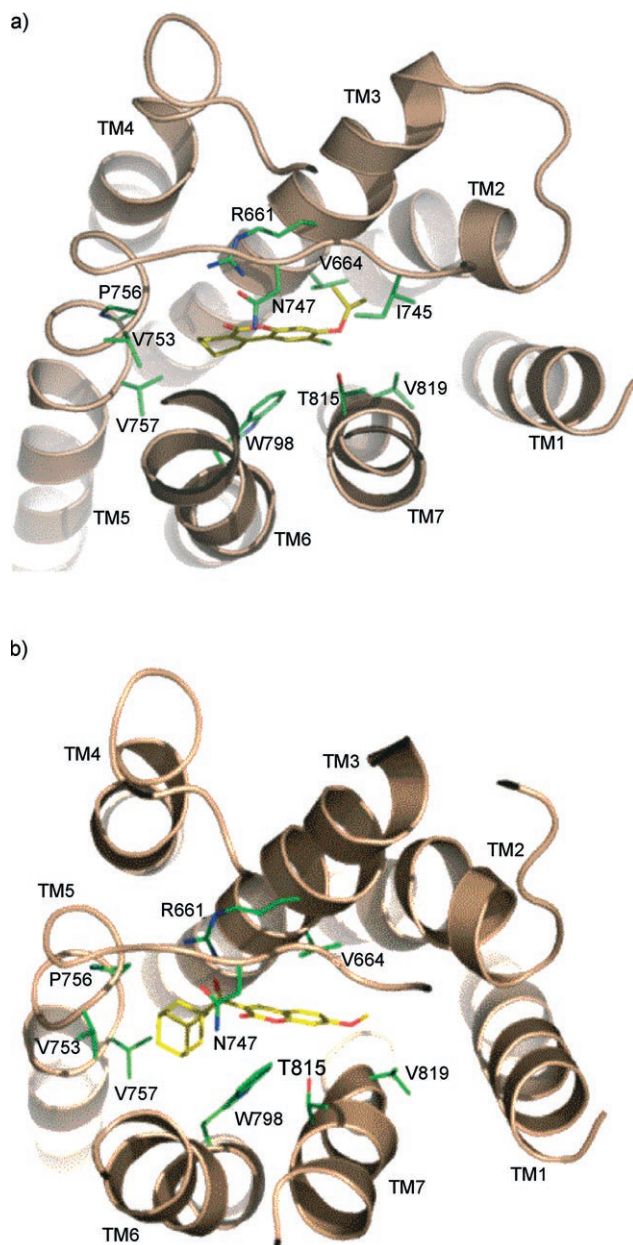


**Figure 5.** a) Potential binding mode of a) **13** and b) **60** in the allosteric binding site of mGluR1, shown from the extracellular side of the membrane

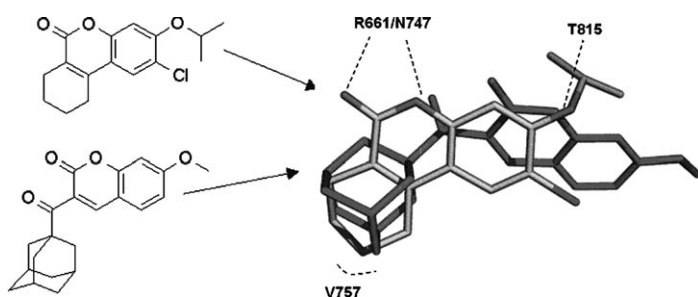


**Figure 6.** Alignment of the structurally different antagonists **13** and **60** and visualization of crucial interaction points within the binding pocket of the mGluR1 homology model.

thesis, Riga, Latvia) for many valuable discussions on this exciting topic. Tobias Noeske thanks Merz Pharmaceuticals GmbH for a PhD grant. This work was supported by the Beilstein Institut zur Förderung der Chemischen Wissenschaften.

**Keywords:** coumarine · GPCR · metabotropic glutamate receptor · pharmacophore descriptors · virtual screening

- [1] J. Wess, *Pharmacol. Ther.* **1998**, *80*, 231.
- [2] A. Christopoulos, T. Kenakin, *Pharmacol. Rev.* **2002**, *54*, 323.
- [3] <http://www.woodmacresearch.com/phview>.
- [4] J. Bockaert, J. P. Pin, *Embo J.* **1999**, *18*, 1723.
- [5] K. A. Jones, B. Borowsky, J. A. Tamm, D. A. Craig, M. M. Durkin, M. Dai, W. J. Yao, M. Johnson, C. Gunwaldsen, L. Y. Huang, C. Tang, Q. Shen, J. A. Salon, K. Morse, T. Laz, K. E. Smith, D. Nagarathnam, S. A. Noble, T. A. Branchek, C. Gerald, *Nature* **1998**, *396*, 674.
- [6] E. M. Brown, G. Gamba, D. Riccardi, M. Lombardi, R. Butters, O. Kifor, A. Sun, M. A. Hediger, J. Lytton, S. C. Hebert, *Nature* **1993**, *366*, 575.
- [7] C. I. Bargmann, *Cell* **1997**, *90*, 585.
- [8] M. A. Hoon, E. Adler, J. Lindemeier, J. F. Battey, N. J. Ryba, C. S. Zuker, *Cell* **1999**, *96*, 541.
- [9] N. Kunishima, Y. Shimada, Y. Tsuji, T. Sato, M. Yamamoto, T. Kumasaka, S. Nakanishi, H. Jingami, K. Morikawa, *Nature* **2000**, *407*, 971.
- [10] J. Wess, *Life Sci.* **1993**, *53*, 1447.
- [11] J. P. Pin, T. Galvez, L. Prezeau, *Pharmacol. Ther.* **2003**, *98*, 325.
- [12] K. Nakamura, T. Nukada, T. Haga, H. Sugiyama, *J. Physiol.* **1994**, *474*, 35.
- [13] F. Nicoletti, V. Bruno, A. Copani, G. Casabona, T. Knopfel, *Trends Neurosci.* **1996**, *19*, 267.
- [14] D. E. Pellegrini-Giampietro, A. Cozzi, F. Peruginelli, P. Leonardi, E. Meli, R. Pellicciari, F. Moroni, *Eur. J. Neurosci.* **1999**, *11*, 3637.
- [15] A. Valerio, M. Paterlini, M. Boifava, M. Memo, P. Spano, *Neuroreport* **1997**, *8*, 2695.
- [16] M. R. Young, S. M. Fleetwood-Walker, R. Mitchell, F. E. Munro, *Neuropharmacology* **1994**, *33*, 141.
- [17] F. Gasparini, R. Kuhn, J. P. Pin, *Curr. Opin. Pharmacol.* **2002**, *2*, 43.
- [18] A. Pagano, D. Ruegg, S. Litschig, N. Stoehr, C. Stierlin, M. Heinrich, P. Floersheim, L. Prezeau, F. Carroll, J. P. Pin, A. Cambria, I. Vranesic, P. J. Flor, F. Gasparini, R. Kuhn, *J. Biol. Chem.* **2000**, *275*, 33750.
- [19] D. Mabire, S. Coupa, C. Adelinet, A. Poncelet, Y. Simonnet, M. Venet, R. Wouters, A. S. Lesage, L. Van Beijsterveldt, F. Bischoff, *J. Med. Chem.* **2005**, *48*, 2134.
- [20] L. Li, R. Tomlinson, Y. Wang, H. C. Tsui, M. Chamberlain, M. Johnson, M. P. Baez, M. Van Nieuwenhze, M. Zia-Ebrahimi, E. J. Hong, *Neuropharmacology* **2002**, *43*, 295.
- [21] P. Malherbe, N. Kratochwil, F. Knoflach, M. T. Zenner, J. N. Kew, C. Kratzeisen, H. P. Maerki, G. Adam, V. Mutel, *J. Biol. Chem.* **2003**, *278*, 8340.
- [22] F. Bordi, A. Ugolini, *Prog. Neurobiol.* **1999**, *59*, 55.
- [23] W. Spooren, T. Ballard, F. Gasparini, M. Amalric, V. Mutel, R. Schreiber, *Behav. Pharmacol.* **2003**, *14*, 257.
- [24] A. S. Lesage, *Current Neuropharmacology* **2004**, *2*, 363.
- [25] G. Schneider, H. J. Böhm, *Drug Discovery Today* **2002**, *7*, 64.
- [26] G. Schneider, W. Neidhart, T. Giller, G. Schmid, *Angew. Chem.* **1999**, *111*, 3068; *Angew. Chem. Int. Ed. Engl.* **1999**, *38*, 2894.
- [27] M. S. Belenikin, G. Costantino, V. A. Palyulin, R. Pellicciari, N. S. Zefirov, *Dokl. Biochem. Biophys.* **2003**, *393*, 341.
- [28] <http://www.asinex.com/prod/gold.html>.
- [29] G. Schneider, P. Schneider, *Drug Discovery* (Eds.: H. Kubinyi, G. Müller), Wiley-VCH, Weinheim, **2004**, 341.
- [30] F. Gasparini, H. Andres, P. J. Flor, M. Heinrich, W. Inderbitzin, K. Lingenhohl, H. Muller, V. C. Munk, K. Omilusik, C. Stierlin, N. Stoehr, I. Vranesic, R. Kuhn, *Bioorg. Med. Chem. Lett.* **2002**, *12*, 407.
- [31] J. R. Hoult, M. Paya, *Gen. Pharmacol.* **1996**, *27*, 713.
- [32] J. A. Ballesteros, H. Weinstein, *Methods in Neuroscience Vol. 25* (Eds.: P. M. Conn, S. C. Sealfon), Academic Press, San Diego, **1995**, 366.
- [33] H. Kwart, E. R. Evans, *J. Org. Chem.* **1966**, *31*, 410.
- [34] M. S. Newman, H. A. Karnes, *J. Org. Chem.* **1966**, *31*, 3980.
- [35] G. Falsone, B. Spur, B. Hundt, *Arch. Pharm.* **1983**, *316*, 960.

- [36] K. Palczewski, T. Kumasaka, T. Hori, C. A. Behnke, H. Motoshima, B. A. Fox, I. Le Trong, D. C. Teller, T. Okada, R. E. Stenkamp, M. Yamamoto, M. Miyano, *Science* **2000**, 289, 739.
- [37] P. Malherbe, N. Kratochwil, M. T. Zenner, J. Piusi, C. Diener, C. Kratzeisen, C. Fischer, R. H. Porter, *Mol. Pharmacol.* **2003**, 64, 823.
- [38] U. Fechner, L. Franke, S. Renner, P. Schneider, G. Schneider, *J. Comput.-Aided Mol. Des.* **2003**, 17, 687.
- [39] O. H. Lowry, N. J. Rosebrough, A. L. Farr, R. J. Randall, *J. Biol. Chem.* **1951**, 193, 265.

---

Received: June 24, 2007

Revised: August 3, 2007

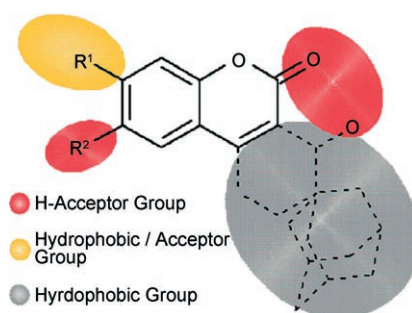
Published online on ■ ■ ■, 2007

## FULL PAPERS

T. Noeske, A. Jirgensons, I. Starchenkova,  
S. Renner, I. Jaunzeme, D. Trifanova,  
M. Hechenberger, T. Bauer, V. Kauss,  
C. G. Parsons, G. Schneider, T. Weil\*



**Virtual Screening for Selective  
Allosteric mGluR1 Antagonists and  
Structure–Activity Relationship  
Investigations for Coumarine  
Derivatives**



**Coumarine mGluR1 antagonists.** The important role of allosteric antagonists of metabotropic glutamate receptors (mGluRs) in diseases involving neurodegeneration, anxiety, pain, epilepsy, neuroprotection, and schizophrenia has been investigated. A virtual screening study and activity optimization program of a series of coumarine derivatives facilitated the discovery of novel and subtype selective noncompetitive antagonists of the mGluR1.